

MRI assessment of cardiac tumours: part 1, multiparametric imaging protocols and spectrum of appearances of histologically benign lesions

Edward T.D. Hoey¹, Muhammad Shahid², Arul Ganeshan¹, Shobhit Bajjal³, Helen Simpson², Richard W. Watkin²

¹Department of Radiology, ²Department of Cardiology, ³Department of Oncology, Heart of England NHS Trust, Birmingham, UK

Correspondence to: Edward T.D. Hoey, MRCP, FRCR. Department of Radiology, Heartlands Hospital, Bordesley Green, Birmingham, B9 5SS, UK. Email: edwardhoey1@gmail.com.

Abstract: Cardiac magnetic resonance imaging (MRI) is the reference standard technique for assessment and characterization of a suspected cardiac tumour. It provides an unrestricted field of view, high temporal resolution and non-invasive tissue characterization based on multi-parametric assessment of the chemical micro-environment. MRI exploits differences in hydrogen proton density in conjunction with T1 and T2 relaxation properties of different tissues to help differentiation normal from abnormal and benign from malignant lesions. In this article we review specific cardiac MRI techniques, tumour protocol design and the appearance of the spectrum of histologically benign tumours.

Keywords: Magnetic resonance imaging (MRI); cardiac tumour; myxoma

Submitted Nov 18, 2014. Accepted for publication Nov 19, 2014.

doi: 10.3978/j.issn.2223-4292.2014.11.23

View this article at: <http://dx.doi.org/10.3978/j.issn.2223-4292.2014.11.23>

Introduction

Cardiac magnetic resonance imaging (MRI) is considered the reference standard technique for characterization of a suspected cardiac mass. It provides an unrestricted field of view, high temporal resolution (30-50 ms) and non-invasive tissue characterization based on multi-parametric assessment of the chemical micro-environment (1). As such MRI is extremely helpful for diagnosis, assessment of the functional impact of a lesion, treatment planning and post treatment follow-up (2). We present a two-part review of the role of cardiac MRI in the assessment of cardiac tumours. Part one focuses on specific cardiac MRI techniques, protocol design and the appearance of histologically benign tumours. Part two covers histologically malignant tumours, and also reviews the MRI appearance of potential tumour mimics.

Primary cardiac tumours are extremely rare with an estimated lifetime incidence across all age groups of 0.0017-0.02% (3,4). Among the primary tumours approximately

75% are benign with more than half of these being myxomas (5). Histologically malignant tumours are predominantly sarcomatous in nature (6-8). By comparison, metastatic involvement of the heart is 100-500 times more frequent than primary tumours (9). Cardiac tumours are frequently asymptomatic and often discovered incidentally during evaluation of an unrelated problem or physical finding. Symptoms and signs depend on the size and location of the tumour, haemodynamic effects (chamber obstruction or embolization) and interference with cardiac conduction (heart blocks or cardiac arrhythmias). Benign primary tumours are often amenable to complete surgical resection with low mortality and morbidity and most patients have a good prognosis if surgery is successful (10). Conversely the prognosis for patients with malignant cardiac sarcomas is dismal with a median survival of only 6-12 months (11), although some may enjoy long-term survival with a radical multidisciplinary approach (12).

Most malignant lesions cannot be completely resected but patients may gain symptomatic benefit from a debulking procedure.

Most cardiac masses are not amenable to percutaneous or catheter biopsy and imaging plays a crucial role in their evaluation. Transthoracic echocardiography (TTE) is usually the first line imaging technique but is often unable to provide complete evaluation due to its limited field of view and limited soft tissue resolution (13). Transesophageal echocardiography (TOE) improves image quality and provides more detailed assessment but also has limited tissue characterization abilities. Multi-detector computed tomography (MDCT) has an emerging role in the assessment of a cardiac mass due to its high spatial resolution (0.4-0.6 mm), short examination time (especially useful in patients with orthopnoea) and ability to definitively detect fat and calcification. Currently the main disadvantage of MDCT is a lack of inherent soft tissue contrast resolution (14,15). Cardiac MRI is considered to be the gold standard technique for assessing a suspected cardiac tumour owing to its unique ability to provide non-invasive tissue characterization in conjunction with high temporal resolution and lack of exposure to ionizing radiation (16,17). In day to day practice echocardiography, MDCT and MRI are frequently used complimentary to one another to provide as much information as possible concerning a suspected cardiac tumour.

Cardiac MRI sequences

A variety of MRI pulse sequences can be used to confirm the presence of a suspected cardiac mass and help assess its tissue composition and impact on adjacent structures including the valves and coronary arteries. MRI exploits differences in hydrogen proton density in conjunction with T1 and T2 relaxation properties of different tissues to help differentiation normal from abnormal and benign from malignant lesions. As malignant cells have a higher free intracellular water content and a greater degree of surrounding extracellular fluid due to interstitial oedema they usually have longer T1 and T2 relaxation times compared with benign pathology (15). Malignant tissue is also associated with a greater degree of neo-angiogenesis and hence first pass contrast enhancement. Necrotic tumour tissue is associated with interstitial expansion and the accumulation and delayed washout of gadolinium based contrast agents (2).

Black blood prepared techniques

“Black-blood” prepared static MRI images are used to help localise a suspected cardiac or juxta cardiac mass and to non-invasively assess its tissue composition. Black blood images are usually acquired using a double-inversion recovery fast spin-echo sequence whereby the initial 180° inversion pulse is non slice selective and followed by a slice-selective 180° pulse (18). This causes blood flowing into the slice to undergo only the first non-selective 180° inversion pulse giving it a black-blood appearance. To achieve T1-weighted images the time to repeat (TR) is set at around 1,000 ms; T2-weighted images require a TR of around 2,000 ms which doubles the acquisition time. The addition of a third slice selective 180° inversion pulse (triple inversion recovery) can be used to give fat saturation which is helpful for characterisation of a fat containing lesion (19).

Bright blood prepared techniques

Cine steady-state free precession (SSFP) is an un-enhanced fast gradient echo technique which uses a short TR (2-3 msec) and segmented k-space filling. SSFP enables cine cardiac imaging at high temporal resolution and at the same time gives excellent contrast definition between the blood pool and myocardium. SSFP has utility for assessing the mobility and attachment point of a mass as well as its dynamic relationship and impact upon the valve structures. SSFP should not be used for assessment of tissue composition of a cardiac mass as its tissue weighting is dependent on both T1 and T2 effects (2,20).

First pass perfusion and delayed enhancement imaging

First pass rest perfusion imaging using a T1-weighted gradient echo sequence and infusion of gadolinium chelate followed by 10-15 minutes delayed enhancement imaging (using a T1-weighted inversion recovery sequence) assesses lesion vascularity. First pass enhancement is typical of highly vascular tumours such as haemangioma or angiosarcoma. The presence of late phase gadolinium enhancement (LGE) implies delayed washout from a lesion, usually as the result of extracellular space expansion or necrosis (21). LGE can be seen with both benign and malignant lesions. Benign tumours like fibroma usually display uniform LGE whereas tumours with a more heterogeneous composition like myxoma or angiosarcoma (containing a mixture of tumour

Table 1 Institutional imaging protocol for assessment of a suspected cardiac tumour

	Sequence name	Scan planes	Parameters	Intravenous contrast	ECG-gating
Structural assessment	T1-weighted double inversion recovery FSE*	Axial: diaphragm to apex; coronal: sternum to spine	TR: 1,000 msec; TE: 35-40 msec; Repletion time: one R-R interval; 6 mm slice thickness	No	Prospective
Tissue characterization	T2-weighted double inversion recovery FSE*	Axial: diaphragm to apex; coronal: sternum to spine	TR: 2,000 msec; TE: 120 msec; Repletion time: two R-R intervals; 6mm slice thickness	No	Prospective
Functional assessment	Steady state free precession	Axial stack: diaphragm to aortic arch; short axis stack; 4-chamber stack; 2-chamber stack	TR: 3-5 msec; TE: 1.5-2 msec; flip angle: 55°; 8 mm slice thickness	No	Retrospective
Rest perfusion study	T1-weighted multi-slice gradient echo	Plane through centre of mass: Mass in LV: short axis; Mass in RV: axial; Mass in LA: axial; Mass in RA: axial	TR: 220 msec; TE: 1.1 msec; flip angle: 50°; 8 mm slice thickness; inversion time set to null normal myocardium (110 msec)	0.05 mmol/kg; Gd-DTPA; @ 5 mL/sec	Prospective
Delayed enhancement study	T1-weighted 2D gradient echo 10-15 min following injection	Axial: diaphragm to apex; coronal: sternum to spine	TR: 450 msec; TE: 1.2 msec; flip angle: 50°; 8 mm slice thickness; inversion time set to null normal myocardium (200-350 msec)	0.1 mmol/kg; Gd-DTPA; @ 1 mL/sec	Prospective

*Repeated with a triple inversion recovery pulse sequence to achieve fat suppression. FSE, fast spin-echo; TR, time to repeat; TE, time to echo; LV, left ventricle; RV, right ventricle; LA, left atrium; RA, right atrium; Gd-DTPA, Gadopentetate dimeglumine.

tissue, necrosis and foci of haemorrhage) usually show patchy LGE (22).

MRI tumour protocol

At our institution cardiac MRI is performed on a 1.5 Tesla scanner (Ingenia, Philips Healthcare, Best, The Netherlands). A summary of our institutional imaging protocol for a suspected cardiac mass is presented in *Table 1*. Black blood images in both the axial and coronal planes are obtained with both T1- and T2-weighting and then followed by fat-suppressed triple inversion recovery images. SSFP sequences are acquired as a contiguous axial plane

stack from the diaphragm to aortic arch as well as along the left ventricular short axis from base to cardiac apex. Additional 2-chamber, 4-chamber and left ventricular outflow tract plane SSFP cines are also acquired to provide optimal assessment of the valves. We then acquire a rest perfusion sequence which is planned through the centre of any mass detected in at least two planes followed by a short stack of LGE images in the same planes.

Benign primary tumours

The approximate frequency of benign primary cardiac tumours presenting in adulthood is presented in *Table 2*.

Table 2 Approximate frequency of both benign and malignant primary cardiac tumors

	Percentage (%)
Benign	
Myxoma	45
Fibroelastoma	15
Lipoma	10
Fibroma	3
Hemangioma	2
Cystic tumour of atrioventricular nodal region	<1
Paraganglioma	<1
Other	<1
Total	75
Malignant	
Angiosarcoma	10
Sarcomas with myofibroblastic differentiation	
Undifferentiated pleomorphic sarcoma	5
Osteosarcoma	1
Leiomyosarcoma	<1
Fibrosarcoma	<1
Liposarcoma	<1
Myofibroblastic tumour	<1
Rhabdomyosarcoma	2
Primary lymphoma	2
Pericardial tumours	
Mesothelioma	2
Synovial sarcoma	<1
Total	25

Most benign tumours are intra-cavitary with a narrow attachment point. Those that arise within the peri- or myocardium are usually well defined, with a homogeneous appearance and narrow zone of transition (23).

Myxoma

Myxoma is the most common primary cardiac neoplasm and is believed to originate from multipotent mesenchymal cell residues within the endocardium (24). Most arise from an area immediately adjacent to the fossa ovalis with a narrow pedicle and villous surface extensions which are friable and at risk of embolization (25). The vast majority develop within

the left atrium and are solitary (26-28). Multiple myxomas are rare and usually seen in association with Carney complex which is an autosomal dominant syndrome characterized by multiple myxomas (including extracardiac myxomas), schwannomas and various endocrine tumours (29,30). Mean age at presentation is 50 years with a slight female predominance (31). Clinical symptoms are wide ranging and may relate to intracardiac obstruction (often mimicking mitral stenosis), systemic embolisation (stroke) or a systemic inflammatory response (arthralgia, fevers) (32-34). Prompt surgical resection of myxoma is advocated for definite diagnosis and to reduce the risk of complications (35-39). The risk of recurrence or development of new lesions is low (estimated at 2-5%) and annual TTE follow-up is recommended for a minimum of 4-year post resection (11).

Typical MRI features are a well-defined spherical or ovoid mobile lobulated mass within either atria, sometimes prolapsing through the atrioventricular valve orifice in diastole. They usually appear hypointense to the blood pool on SSFP sequences (2). T1 and T2-weighted images usually show a heterogeneous appearance because of the combination of tumour tissue, necrotic elements and foci of haemorrhage and calcification (40-42) (*Figure 1*). First pass perfusion is usually absent and LGE is often multi-focal and patchy although may sometimes be homogeneous.

The main imaging differential for myxoma is thrombus. Key discriminating features which are usually reliable for distinguishing thrombus from myxoma are an absence of LGE and lack of atrioventricular valve prolapse (43).

Papillary fibroelastoma

Fibroelastoma is the most common primary tumour of the cardiac valves although may arise from any endocardial surface (44). They are usually small lesions (<1.5 cm) and are composed of collagen and elastic tissue fibres lined by endothelium with a short pedicle (45). Commonest sites are the atrial side of the mitral valve and aortic surface of the aortic valve leaflets. The majority are asymptomatic and observed serendipitously at TTE performed for another reason but on occasion they may cause symptoms as a result of embolization of tumour fragments or surface thrombus into the systemic or pulmonary circulations (45). Aortic valve fibroelastomas can rarely be a cause of sudden death due to presumed acute obstruction of the coronary artery ostia (46). Prompt surgical resection is the treatment of choice, especially for left sided lesions (40).

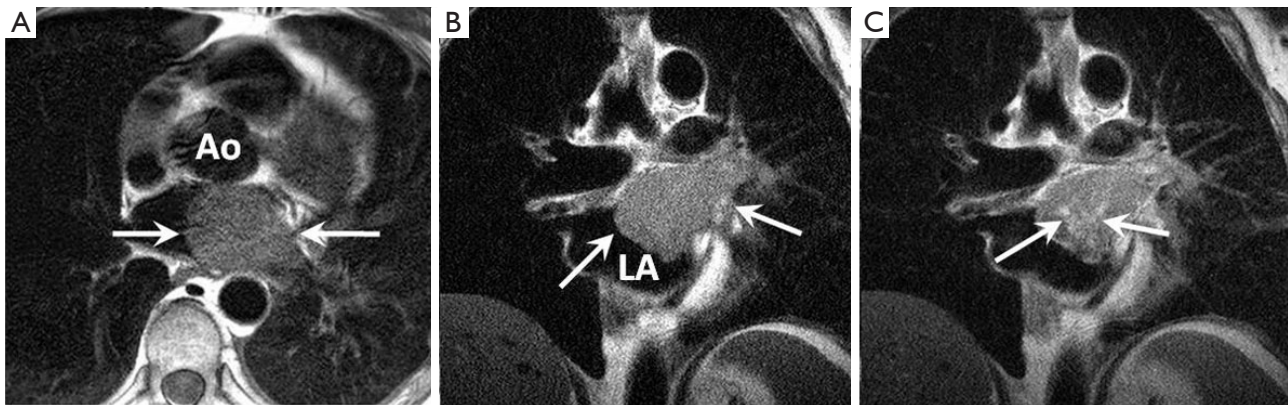


Figure 1 Large left atrial/left atrial appendage myxoma. (A) Axial T1-weighted black blood image showing a well-defined slightly heterogeneous signal lesion within the body of the left atrium (arrows); (B) coronal T1-weighted black blood image showing the myxoma filling the left atrial appendage and filling a large portion of the left atrium (arrows); (C) coronal T1-weighted delayed phase image acquired 15 minutes post gadolinium showing patchy central foci of enhancement (arrows). Ao, aorta; LA, left atrium.

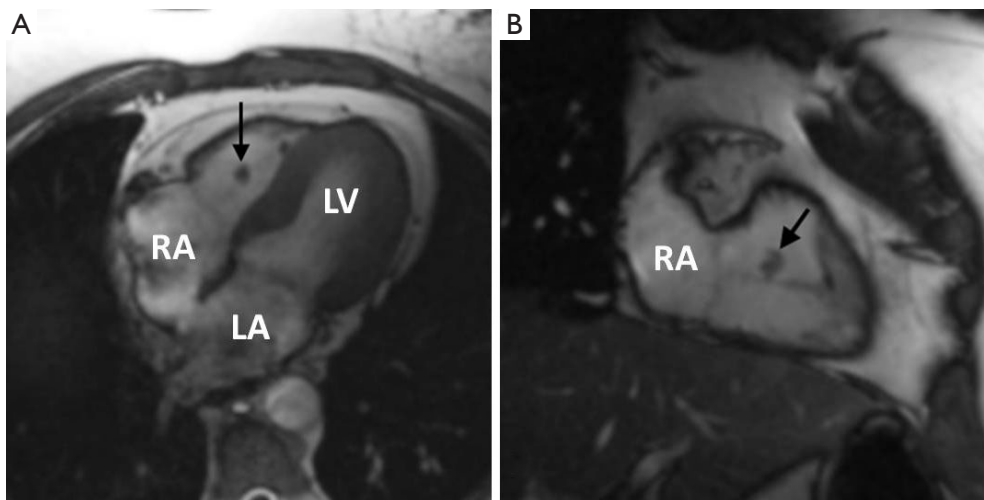


Figure 2 Fibroelastoma of the tricuspid sub-valvular apparatus. (A) 4-chamber SSFP image showing a well circumscribed small nodule within the body of the right ventricle (arrow). This lesion was highly mobile on cine review; (B) 2-chamber SSFP image through the right heart chambers showing the fibroelastoma attached to the valvular chordae via a thin stalk (arrow). RA, right atrium; LA, left atrium; LV, left ventricle.

TOE is the modality of choice to detect these small highly mobile lesions and MRI is rarely required. When imaged with MRI features are those of a low signal well circumscribed mobile valve nodule on SSFP sequences, often with peri-lesional flow artifact (47-49) (*Figure 2*). T1 and T2 weighted images reflect their fibroelastic composition with uniform intermediate signal intensity similar to myocardium. Homogeneous LGE has been reported but in our experience LGE is commonly absent in keeping with a poorly vascularised lesion (50). The main

imaging differential is a vegetation of infective endocarditis but distinction is generally straightforward on clinical grounds. On imaging vegetations are invariably associated with valve destruction/incompetence unlike a fibroelastoma with which valve function is usually preserved (51).

Lipoma

Lipomas are an encapsulated conglomerate of slow growing mature adipose tissue. They can occur anywhere

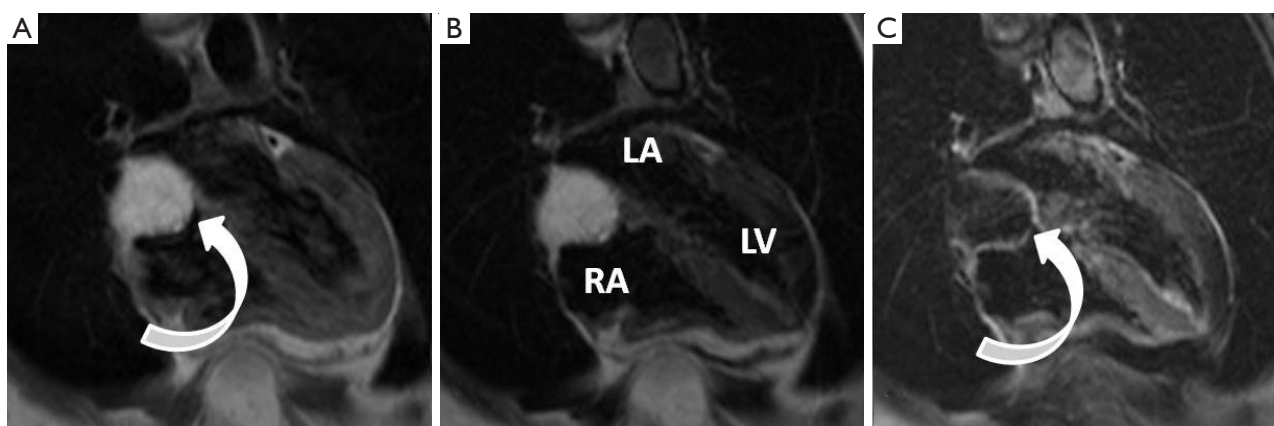


Figure 3 Atrial septal lipoma. (A) 4-Chamber T2-weighted black blood image showing a well-defined uniformly high signal lesion within the interatrial septum (curved arrow); (B) 4-Chamber T1-weighted black blood image again showing the lesion as having uniformly high signal in keeping with a fat composition; (C) 4-Chamber T2-weighted black blood image with fat suppression showing complete and uniform signal suppression (curved arrow). RA, right atrium; LA, left atrium; LV, left ventricle.

in the heart but are most frequently seen within the atrial septum and epicardium where they grow into the pericardial space. Subendocardial lipomas are broad based lesions which protrude into the cardiac chambers and may cause obstructive and compressive effects but most probably remain asymptomatic and are discovered incidentally (52-54). There is a reported association with atrial arrhythmias and conduction abnormalities. Surgical resection is rarely needed except with very large and symptomatic lesions (40).

Lipomatous hypertrophy of the inter-atrial septum is hyperplasia of normal septal fat and also reflects a benign entity. The key distinguishing feature from lipoma is sparing of the mid-septal region (fossa ovalis) giving rise to their classical “dumbbell” appearance.

Lipomas and lipomatous hypertrophy have a highly variable appearance on echocardiography making confident distinction from other cardiac tumours like myxoma challenging (55). MRI appearances are typical owing to definitive characterization of fat signal which appears of uniformly high signal on both T1 and T2-weighted imaging and fully suppresses with fat saturation (*Figure 3*). Due to their avascular nature there is no first pass or LGE with these lesions (56).

Haemangioma

These are slow flow vascular malformations composed of endothelial lined venous channels with an intervening

connective tissue stroma (56). There is no chamber predilection and they have been described in many locations including within the pericardial space. Most probably remain asymptomatic but large lesions are associated with exertional dyspnoea and may be considered for surgical resection.

On MRI they display isointense signal to myocardium on T1-weighted images due to slow flow and of diffuse high signal intensity on T2-weighted images. First pass and delayed enhancement is intense and prolonged and may appear heterogeneous depending upon the amount of fibrous tissue and any calcific foci (57).

Fibroma

Fibromas are the most common paediatric cardiac tumour but they are occasionally seen in adults (58-60). Typically, they have an intramural location within the interventricular septum or left ventricular free wall (61). Fibromas have been associated with Polyposis syndromes (familial adenomatous polyposis) and Gorlin-Goltz syndrome (62,63). Histologically they are well-defined lesions composed of collagen and fibroblasts with some calcific foci which help differentiate them from rhabdomyomas. Heart failure is the most common clinical presentation due to obstruction of blood flow or interference with valvular function. Ventricular arrhythmias and sudden death have also been reported (63).

On MRI fibromas are usually sharply demarcated and

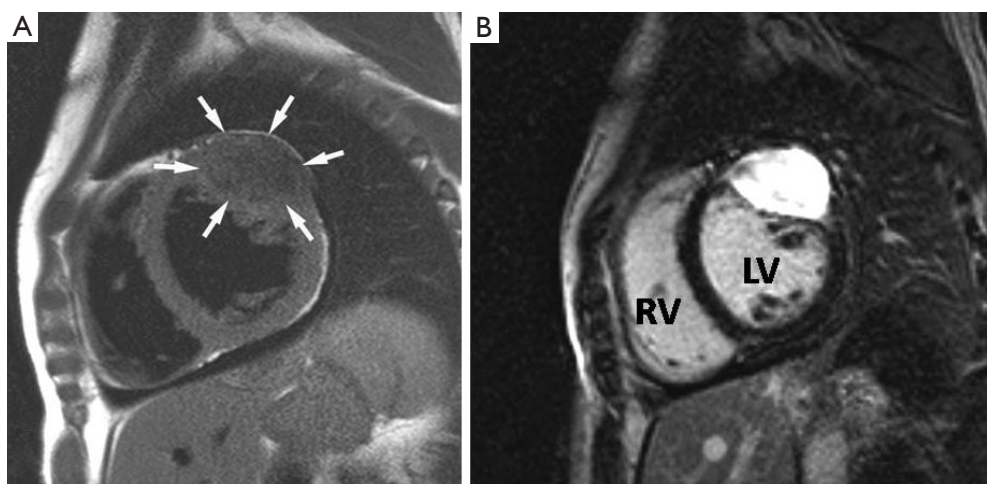


Figure 4 Left ventricular fibroma. (A) Short axis mid left ventricle T1-weighted image showing a well-defined uniformly low signal mass within the anterolateral wall (arrows); (B) short axis mid left ventricle T1-weighted image obtained 10 minutes post gadolinium administration showing uniform intense enhancement. RV, right ventricle; LV, left ventricle.

of uniformly low signal intensity compared with adjacent myocardium on both T1 and T2-weighted imaging due to their dense fibrous composition (64). A lack of first pass enhancement is typical and LGE is commonly intense and uniform although peripheral and heterogenous LGE patterns have also been described (65,66) (*Figure 4*). The main imaging differential of a fibroma with little or no delayed enhancement is focal hypertrophic cardiomyopathy and distinction can be challenging. Careful review of the cine images is the best means of discrimination with a fibroma showing no regions of contractility which can usually be appreciated in most cases of “mass-like” hypertrophic cardiomyopathy (65).

Cardiac paraganglioma

Paraganglioma is a very rare tumour which originates from neuroendocrine ganglia cells which tend to lie within the atrioventricular grooves and at the root of the great vessel origins (67). Up to 50% of these tumours secrete catecholamines which explains the typical clinical presentation of palpitations, flushing and headaches. Patients may also be hypertensive. Although histologically benign curative resection is often difficult due to extensive vascularity and often complex relationship with the adjacent coronary arteries.

On MRI these lesions usually range in size from 4-8 cm appearing well circumscribed. They are isointense to myocardium on T1- and of intensely high signal on T2-

weighted images (“light bulb bright”) (*Figure 5*). First pass and LGE is usually intense and uniform (23).

Cystic tumour of the atrioventricular node

This is one of the rarest benign cardiac tumours with only a few cases reported in the literature. It is postulated to be an inclusion cyst of endodermal origin containing keratinous debris. Most reported lesions are small (<2 cm) and located at the base of the interatrial septum in the atrioventricular nodal region where they may cause interference with cardiac conduction leading to heart block and potentially lethal arrhythmias. Surgical resection is therefore advocated (68,69).

Described MRI features are those of a well-defined high T1 and high T2-signal nodule in the AV nodal region of the lower septum (*Figure 6*). Homogeneous LGE has been reported (70).

Conclusions

A comprehensive cardiac tumour imaging protocol has been described and the spectrum of benign primary tumour MRI appearances has been reviewed. Part 2 of this review will focus on primary malignant cardiac tumours, cardiac metastases as well as the MRI features of some potential tumour mimics.

Disclosure: The authors declare no conflict of interest.

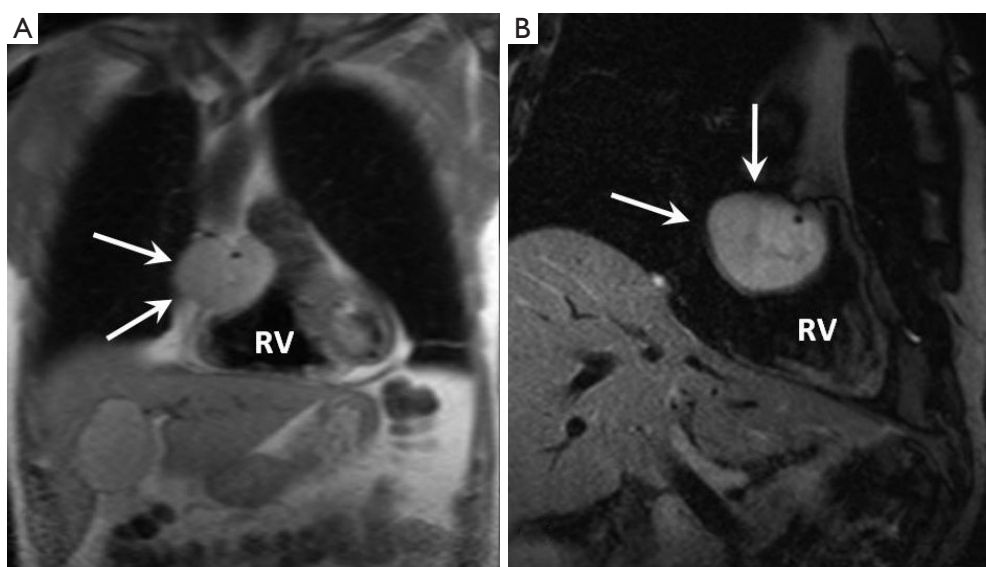


Figure 5 Cardiac paraganglioma. (A) Coronal T1-weighted black blood image showing a well-defined intermediate signal lesion at the root of the great vessels and indenting the roof of the right ventricle (arrows); (B) coronal T2-weighted black blood image showing the lesion to be of intensely high signal (arrows). RV, right ventricle.

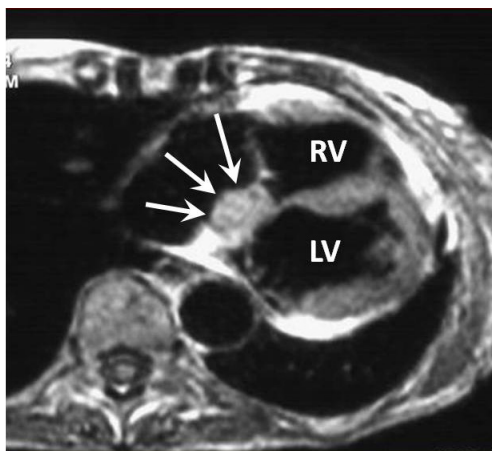


Figure 6 Cystic atrioventricular nodal tumour. Axial T1-weighted black blood image showing a well-defined uniformly high signal lesion within the lower margin of the interatrial septum (arrows). RV, right ventricle; LV, left ventricle.

References

1. Kaminaga T, Takeshita T, Kimura I. Role of magnetic resonance imaging for evaluation of tumors in the cardiac region. *Eur Radiol* 2003;13 Suppl 4:L1-10.
2. Sparrow PJ, Kurian JB, Jones TR, Sivananthan MU. MR imaging of cardiac tumors. *Radiographics* 2005;25:1255-76.
3. Reynen K. Frequency of primary tumors of the heart. *Am J Cardiol* 1996;77:107.
4. Centofanti P, Di Rosa E, Deorsola L, Dato GM, Patanè F, La Torre M, Barbato L, Verzini A, Fortunato G, di Summa M. Primary cardiac tumors: early and late results of surgical treatment in 91 patients. *Ann Thorac Surg* 1999;68:1236-41.
5. Lam KY, Dickens P, Chan AC. Tumors of the heart. A 20-year experience with a review of 12,485 consecutive autopsies. *Arch Pathol Lab Med* 1993;117:1027-31.
6. Molina JE, Edwards JE, Ward HB. Primary cardiac tumors: experience at the University of Minnesota. *Thorac Cardiovasc Surg* 1990;38 Suppl 2:183-91.
7. Orlandi A, Ferlosio A, Roselli M, Chiariello L, Spagnoli LG. Cardiac sarcomas: an update. *J Thorac Oncol* 2010;5:1483-9.
8. Simpson L, Kumar SK, Okuno SH, Schaff HV, Porrata LF, Buckner JC, Moynihan TJ. Malignant primary cardiac tumors: review of a single institution experience. *Cancer* 2008;112:2440-6.
9. Chiles C, Woodard PK, Gutierrez FR, Link KM. Metastatic involvement of the heart and pericardium: CT and MR imaging. *Radiographics* 2001;21:439-49.
10. Bakaeen FG, Reardon MJ, Coselli JS, Miller CC, Howell JF, Lawrie GM, Espada R, Ramchandani MK, Noon GP, Weillbaeher DG, DeBaKey ME. Surgical outcome in 85 patients with primary cardiac tumors. *Am J Surg*

- 2003;186:641-7; discussion 647.
11. Donsbeck AV, Ranchere D, Coindre JM, Le Gall F, Cordier JF, Loire R. Primary cardiac sarcomas: an immunohistochemical and grading study with long-term follow-up of 24 cases. *Histopathology* 1999;34:295-304.
 12. Shapira OM, Korach A, Izhar U, Koler T, Wald O, Ayman M, Erez E, Blackmon SH, Reardon MJ. Radical multidisciplinary approach to primary cardiac sarcomas. *Eur J Cardiothorac Surg* 2013;44:330-5; discussion 335-6.
 13. Süttsch G, Jenni R, von Segesser L, Schneider J. Heart tumors: incidence, distribution, diagnosis. Exemplified by 20,305 echocardiographies. *Schweiz Med Wochenschr* 1991;121:621-9.
 14. Roberts WT, Bax JJ, Davies LC. Cardiac CT and CT coronary angiography: technology and application. *Heart* 2008;94:781-92.
 15. Mitchell DG, Burk DL Jr, Vinitzki S, Rifkin MD. The biophysical basis of tissue contrast in extracranial MR imaging. *AJR Am J Roentgenol* 1987;149:831-7.
 16. Bluemke DA, Achenbach S, Budoff M, Gerber TC, Gersh B, Hillis LD, Hundley WG, Manning WJ, Printz BF, Stuber M, Woodard PK. Noninvasive coronary artery imaging: magnetic resonance angiography and multidetector computed tomography angiography: a scientific statement from the american heart association committee on cardiovascular imaging and intervention of the council on cardiovascular radiology and intervention, and the councils on clinical cardiology and cardiovascular disease in the young. *Circulation* 2008;118:586-606.
 17. Pennell DJ, Sechtem UP, Higgins CB, Manning WJ, Pohost GM, Rademakers FE, van Rossum AC, Shaw LJ, Yucel EK; Society for Cardiovascular Magnetic Resonance; Working Group on Cardiovascular Magnetic Resonance of the European Society of Cardiology. Clinical indications for cardiovascular magnetic resonance (CMR): Consensus Panel report. *Eur Heart J* 2004;25:1940-65.
 18. Stehling MK, Holzknacht NG, Laub G, Böhm D, von Smekal A, Reiser M. Single-shot T1- and T2-weighted magnetic resonance imaging of the heart with black blood: preliminary experience. *MAGMA* 1996;4:231-40.
 19. Simonetti OP, Finn JP, White RD, Laub G, Henry DA. "Black blood" T2-weighted inversion-recovery MR imaging of the heart. *Radiology* 1996;199:49-57.
 20. Hansen MW, Merchant N. MRI of hypertrophic cardiomyopathy: part I, MRI appearances. *AJR Am J Roentgenol* 2007;189:1335-43.
 21. Kramer CM, Barkhausen J, Flamm SD, Kim RJ, Nagel E; Society for Cardiovascular Magnetic Resonance Board of Trustees Task Force on Standardized Protocols. Standardized cardiovascular magnetic resonance imaging (CMR) protocols, society for cardiovascular magnetic resonance: board of trustees task force on standardized protocols. *J Cardiovasc Magn Reson* 2008;10:35.
 22. Hoffmann U, Globits S, Schima W, Loewe C, Puig S, Oberhuber G, Frank H. Usefulness of magnetic resonance imaging of cardiac and paracardiac masses. *Am J Cardiol* 2003;92:890-5.
 23. Reynen K. Cardiac myxomas. *N Engl J Med* 1995;333:1610-7.
 24. Kono T, Koide N, Hama Y, Kitahara H, Nakano H, Suzuki J, Isobe M, Amano J. Expression of vascular endothelial growth factor and angiogenesis in cardiac myxoma: a study of fifteen patients. *J Thorac Cardiovasc Surg* 2000;119:101-7.
 25. Hoey ET, Mankad K, Puppala S, Gopalan D, Sivananthan MU. MRI and CT appearances of cardiac tumours in adults. *Clin Radiol* 2009;64:1214-30.
 26. Carney JA, Hruska LS, Beauchamp GD, Gordon H. Dominant inheritance of the complex of myxomas, spotty pigmentation, and endocrine overactivity. *Mayo Clin Proc* 1986;61:165-72.
 27. Pinede L, Duhaut P, Loire R. Clinical presentation of left atrial cardiac myxoma. A series of 112 consecutive cases. *Medicine (Baltimore)* 2001;80:159-72.
 28. Tazelaar HD, Locke TJ, McGregor CG. Pathology of surgically excised primary cardiac tumors. *Mayo Clin Proc* 1992;67:957-65.
 29. Carney JA, Gordon H, Carpenter PC, Shenoy BV, Go VL. The complex of myxomas, spotty pigmentation, and endocrine overactivity. *Medicine (Baltimore)* 1985;64:270-83.
 30. Casey M, Mah C, Merliss AD, Kirschner LS, Taymans SE, Denio AE, Korf B, Irvine AD, Hughes A, Carney JA, Stratakis CA, Basson CT. Identification of a novel genetic locus for familial cardiac myxomas and Carney complex. *Circulation* 1998;98:2560-6.
 31. Burke A, Virmani R. Tumors of the heart and great vessels. In: *Atlas of tumor pathology: fasc 16, ser 3*. Washington, DC: Armed Forces Institute of Pathology, 1996:1-98.
 32. Markel ML, Waller BF, Armstrong WF. Cardiac myxoma. A review. *Medicine (Baltimore)* 1987;66:114-25.
 33. Eckhardt BP, Dommann-Scherrer CC, Stuckmann G, Zollikofer CL, Wentz KU. Giant cardiac myxoma with malignant transformed glandular structures. *Eur Radiol* 2003;13:2099-102.
 34. Todo T, Usui M, Nagashima K. Cerebral metastasis of malignant cardiac myxoma. *Surg Neurol* 1992;37:374-9.

35. Keeling IM, Oberwalder P, Anelli-Monti M, Schuchlenz H, Demel U, Tilz GP, Rehak P, Rigler B. Cardiac myxomas: 24 years of experience in 49 patients. *Eur J Cardiothorac Surg* 2002;22:971-7.
36. Selkane C, Amahzoune B, Chavanis N, Raisky O, Robin J, Ninet J, Obadia JF. Changing management of cardiac myxoma based on a series of 40 cases with long-term follow-up. *Ann Thorac Surg* 2003;76:1935-8.
37. Cina SJ, Smialek JE, Burke AP, Virmani R, Hutchins GM. Primary cardiac tumors causing sudden death: a review of the literature. *Am J Forensic Med Pathol* 1996;17:271-81.
38. Jelic J, Milicić D, Alfirević I, Anić D, Baudoin Z, Bulat C, Corić V, Dadić D, Husar J, Ivančan V, Korda Z, Letica D, Predrijevac M, Ugljen R, Vućemilo I. Cardiac myxoma: diagnostic approach, surgical treatment and follow-up. A twenty years experience. *J Cardiovasc Surg (Torino)* 1996;37:113-7.
39. Bakaeen FG, Reardon MJ, Coselli JS, Miller CC, Howell JF, Lawrie GM, Espada R, Ramchandani MK, Noon GP, Weilbaeher DG, DeBakey ME. Surgical outcome in 85 patients with primary cardiac tumors. *Am J Surg* 2003;186:641-7; discussion 647.
40. Bruce CJ. Cardiac tumours: diagnosis and management. *Heart* 2011;97:151-60.
41. Singh SD, Lansing AM. Familial cardiac myxoma--a comprehensive review of reported cases. *J Ky Med Assoc* 1996;94:96-104.
42. Schwartzman PR, White RD. Imaging of cardiac and paracardiac masses. *J Thorac Imaging* 2000;15:265-73.
43. Scheffel H, Baumüller S, Stolzmann P, Leschka S, Plass A, Alkadhi H, Schertler T. Atrial myxomas and thrombi: comparison of imaging features on CT. *AJR Am J Roentgenol* 2009;192:639-45.
44. van Werkum MH, Swaans MJ, van Es HW, Rensing B, van Heeswijk JP. Case 190: papillary fibroelastoma of the pulmonary valve. *Radiology* 2013;266:680-4.
45. Sun JP, Asher CR, Yang XS, Cheng GG, Scalia GM, Massed AG, Griffin BP, Ratliff NB, Stewart WJ, Thomas JD. Clinical and echocardiographic characteristics of papillary fibroelastomas: a retrospective and prospective study in 162 patients. *Circulation* 2001;103:2687-93.
46. Wintersperger BJ, Becker CR, Gulbins H, Knez A, Bruening R, Heuck A, Reiser MF. Tumors of the cardiac valves: imaging findings in magnetic resonance imaging, electron beam computed tomography, and echocardiography. *Eur Radiol* 2000;10:443-9.
47. Sengupta PP, Khandheria BK. Transoesophageal echocardiography. *Heart* 2005;91:541-7.
48. Kondruweit M, Schmid M, Strecker T. Papillary fibroelastoma of the mitral valve: appearance in 64-slice spiral computed tomography, magnetic resonance imaging, and echocardiography. *Eur Heart J* 2008;29:831.
49. Syed IS, Feng D, Harris SR, Martinez MW, Misselt AJ, Breen JF, Miller DV, Araoz PA. MR imaging of cardiac masses. *Magn Reson Imaging Clin N Am* 2008;16:137-64, vii.
50. Kelle S, Chiribiri A, Meyer R, Fleck E, Nagel E. Images in cardiovascular medicine. Papillary fibroelastoma of the tricuspid valve seen on magnetic resonance imaging. *Circulation* 2008;117:e190-1.
51. Klarich KW, Enriquez-Sarano M, Gura GM, Edwards WD, Tajik AJ, Seward JB. Papillary fibroelastoma: echocardiographic characteristics for diagnosis and pathologic correlation. *J Am Coll Cardiol* 1997;30:784-90.
52. Friedberg MK, Chang IL, Silverman NH, Ramamoorthy C, Chan FP. Images in cardiovascular medicine. Near sudden death from cardiac lipoma in an adolescent. *Circulation* 2006;113:e778-9.
53. Puvanewary M, Edwards JR, Bastian BC, Khatri SK. Pericardial lipoma: ultrasound, computed tomography and magnetic resonance imaging findings. *Australas Radiol* 2000;44:321-4.
54. Lang-Lazdunski L, Oroudji M, Pansard Y, Visuzaine C, Hvass U. Successful resection of giant intrapericardial lipoma. *Ann Thorac Surg* 1994;58:238-40; discussion 240-1.
55. Restrepo CS, Largoza A, Lemos DF, Diethelm L, Koshy P, Castillo P, Gomez R, Moncada R, Pandit M. CT and MR imaging findings of benign cardiac tumors. *Curr Probl Diagn Radiol* 2005;34:12-21.
56. Grebenc ML, Rosado de Christenson ML, Burke AP, Green CE, Galvin JR. Primary cardiac and pericardial neoplasms: radiologic-pathologic correlation. *Radiographics* 2000;20:1073-103; quiz 1110-1, 1112.
57. Oshima H, Hara M, Kono T, Shibamoto Y, Mishima A, Akita S. Cardiac hemangioma of the left atrial appendage: CT and MR findings. *J Thorac Imaging* 2003;18:204-6.
58. ElBardissi AW, Dearani JA, Daly RC, Mullany CJ, Orszulak TA, Puga FJ, Schaff HV. Analysis of benign ventricular tumors: long-term outcome after resection. *J Thorac Cardiovasc Surg* 2008;135:1061-8.
59. Valente M, Cocco P, Thiene G, Casula R, Poletti A, Milanese O, Fasoli G, Livi U. Cardiac fibroma and heart transplantation. *J Thorac Cardiovasc Surg* 1993;106:1208-12.
60. Burke AP, Rosado-de-Christenson M, Templeton PA, Virmani R. Cardiac fibroma: clinicopathologic correlates and surgical treatment. *J Thorac Cardiovasc Surg* 1994;108:862-70.

61. Cho JM, Danielson GK, Puga FJ, Dearani JA, McGregor CG, Tazelaar HD, Hagler DJ. Surgical resection of ventricular cardiac fibromas: early and late results. *Ann Thorac Surg* 2003;76:1929-34.
62. Yang HS, Arabia FA, Chaliki HP, De Petris G, Khandheria BK, Chandrasekaran K. Images in cardiovascular medicine. Left atrial fibroma in gardner syndrome: real-time 3-dimensional transesophageal echo imaging. *Circulation* 2008;118:e692-6.
63. Herman TE, Siegel MJ, McAlister WH. Cardiac tumor in Gorlin syndrome. Nevroid basal cell carcinoma syndrome. *Pediatr Radiol* 1991;21:234-5.
64. Brechtel K, Reddy GP, Higgins CB. Cardiac fibroma in an infant: magnetic resonance imaging characteristics. *J Cardiovasc Magn Reson* 1999;1:159-61.
65. O'Donnell DH, Abbara S, Chaithiraphan V, Yared K, Killeen RP, Cury RC, Dodd JD. Cardiac tumors: optimal cardiac MR sequences and spectrum of imaging appearances. *AJR Am J Roentgenol* 2009;193:377-87.
66. Kiaffas MG, Powell AJ, Geva T. Magnetic resonance imaging evaluation of cardiac tumor characteristics in infants and children. *Am J Cardiol* 2002;89:1229-33.
67. Manger WM. An overview of pheochromocytoma: history, current concepts, vagaries, and diagnostic challenges. *Ann N Y Acad Sci* 2006;1073:1-20.
68. Kaminishi Y, Watanabe Y, Nakata H, Shimokama T, Jikuya T. Cystic tumor of the atrioventricular nodal region. *Jpn J Thorac Cardiovasc Surg* 2002;50:37-9.
69. Butany J, Nair V, Naseemuddin A, Nair GM, Catton C, Yau T. Cardiac tumours: diagnosis and management. *Lancet Oncol* 2005;6:219-28.
70. Tran TT, Starnes V, Wang X, Getzen J, Ross BD. Cardiovascular magnetic resonance diagnosis of cystic tumor of the atrioventricular node. *J Cardiovasc Magn Reson* 2009;11:13.

Cite this article as: Hoey ET, Shahid M, Ganeshan A, Baijal S, Simpson H, Watkin RW. MRI assessment of cardiac tumours: part 1, multiparametric imaging protocols and spectrum of appearances of histologically benign lesions. *Quant Imaging Med Surg* 2014;4(6):478-488. doi: 10.3978/j.issn.2223-4292.2014.11.23